

Thermodynamic properties of the $SO(5)$ theory for the antiferromagnetism and d -wave superconductivity: a Monte Carlo study

Xiao Hu

National Research Institute for Metals, Tsukuba 305-0047, Japan

(submitted to Phys. Rev. B on February 8, 2020)

Thermodynamic properties of the $SO(5)$ theory unifying the antiferromagnetism (AF) and the d -wave superconductivity (SC) are explored by means of Monte Carlo simulations on a classical model hamiltonian. The present approach takes into account thermal fluctuations both in the rotation of $SO(5)$ superspins between the AF and SC subspaces, and in the phase variables of SC order parameters. Temperature vs. g -field phase diagrams for null external magnetic field are presented, where the g field is conjugate with the quadratic order parameters and breaks the $SO(5)$ symmetry. The normal(N)/AF and N/SC phase boundaries, both associated with second-order phase transitions, merge tangentially at the bicritical point into the first-order AF/SC phase boundary. Hysteresis phenomenon is observed at the AF/SC phase transition, and therefore the present study suggests the existence of a phase-separation region in the phase diagram. Enhancement of AF correlations is observed above the SC critical temperature near the bicritical point in systems with AF couplings stronger than SC ones. Its relation with the spin-gap phenomenon is addressed. The $SO(5)$ theory in an external magnetic field is also investigated, and the following properties are clarified: At sufficiently large g fields the SC order is established through a first-order freezing transition from the flux-line liquid into the flux-line lattice. Short-range AF fluctuations are larger at cores of flux lines than elsewhere, and decrease continuously to zero with increasing g field. At intermediate g fields, the flux-line lattice of long-range SC order and the long-range AF order coexist. Superlattice spots surrounding the strong AF Bragg peaks at $Q = (\pm\pi, \pm\pi)$ are observed in the simulated structure factor, and are identified with the modulation by the triangular flux-line lattice of SC. The AF phase boundary associated with the continuous onset of long-range AF order drops sharply to the g axis from a finite temperature in the temperature vs. g -field phase diagram.

PACS numbers: 74.25.Dw, 05.50.+q, 74.20.-z, 74.25.Ha

I. INTRODUCTION

High- T_c superconductivity (SC) in cuprates [1] is achieved by hole doping from the insulating state of antiferromagnetism (AF). The AF and SC phases are proximate each other in temperature vs. hole-doping-rate phase diagrams. Enhancement of AF correlations is observed above the SC transition temperature in the underdoped region [2]. A clear signal from these experimental facts is the importance of the inter-relationship between these two very different and even expelling, at a first glance, properties. To explain theoretically the complex phase diagrams of the high- T_c SC is still very challenging for the condensed matter physics. This problem has been approached using microscopic models, such as Hubbard hamiltonian and the simplified $t - J$ hamiltonian [3,4]. It has been tried to derive microscopically the attractive force necessary for Cooper-pair formation from the magnetic interactions, and to construct the phase diagram with the AF and SC phases side by side. Up to date, however, there is no well accepted microscopic theory which can count for the most important features of the high- T_c SC both qualitatively and quantitatively.

In the $SO(5)$ theory this problem is approached in another way [5,6]: The long-range SC and AF orders are presumed as the two possible long-range orders in pure systems. The three components of the AF order parameter and the real and imaginary parts of the SC order parameter compose a five-component superspin of $SO(5)$ symmetry. At low temperatures the $SO(5)$ symmetry is broken into two subspaces, the $SO(3)$ one associated with AF, and the $U(1)$ one associated with SC. The destination of the broken symmetry is controlled by the doping rate, or the chemical potential of holes. Therefore, the doping rate plays the role of $SO(5)$ -symmetry breaking field. Much interest has been stimulated by the proposal of the $SO(5)$ theory, and considerable progresses in exploring this theory have been achieved [7–15]. Since the superspin vector in the $SO(5)$ theory is of five dimensions, three for AF and two for SC, entropy effects on the competition between these two long-range orders are highly nontrivial. Thermal fluctuations are very crucial in determining phase diagrams [13]. Therefore, investigation of the $SO(5)$ theory at finite temperatures is essential for a comprehensive understanding of the theory. Ultimately one should compare the predictions by the theory with phase diagrams observed experimentally. The $SO(5)$ theory also raises interests in the point of view of phase transitions and critical phenomena. To reveal the thermodynamic properties of the $SO(5)$ theory is the objective of the present study. Another important issue is the competition between the long-range SC order in the presence of an external magnetic field, realized in the flux-line lattice (FLL), and the long-range AF order. Since many interesting magnetic-field responses have been clarified in the long-range AF and SC orders separately, the proximity of them in high- T_c cuprates is very likely to produce more sophisticated phenomena. Actually, it is suggested that vortices induced by an external magnetic field in high- T_c superconductors may possess AF cores [5]. To explore the vortex states in high- T_c cuprates in the scheme of $SO(5)$ theory is also very important.

In order to achieve the above purposes, Monte Carlo simulations on a classical model hamiltonian in three-dimensional (3D) space are performed [13]. The present approach takes into account thermal fluctuations both in the rotation of $SO(5)$ superspins between the AF and SC subspaces, and in the phase variables of SC order parameters. The remainder of this paper is organized as follows: The hamiltonian is presented in Sec. II, with descriptions on

technical details of simulation. In Sec. III, simulation results for the null external magnetic field are presented. There are the AF, AF and SC phase-separation, and SC phases in the phase diagrams. The spin-gap phenomenon is also addressed. Section IV is devoted to reveal the effects of an external magnetic field in the $SO(5)$ theory. Coexistence between the long-range AF order and the FLL of long-range SC order is observed. Vortex cores are found of larger AF components than elsewhere. Summary is given in Sec. V.

II. HAMILTONIAN AND SIMULATION TECHNIQUES

The hamiltonian in the present study is given by

$$\mathcal{H} = - \sum_{\langle i,j \rangle} J_{i,j}^{SC} \mathbf{t}_i \cdot \mathbf{t}_j + \sum_{\langle i,j \rangle} J_{i,j}^{AF} \mathbf{s}_i \cdot \mathbf{s}_j + g \sum_i \mathbf{s}_i^2, \quad (1)$$

defined on the simple cubic lattice. The vector \mathbf{t} , of two components and coupling ferromagnetically with nearest neighbors, is for the d -wave SC order parameter; the vector \mathbf{s} , of three components and with AF coupling between nearest neighbors, is for the AF order parameter. The interplay between the SC and AF order parameters is introduced by the $SO(5)$ constraint on the superspin:

$$\mathbf{s}_i^2 + \mathbf{t}_i^2 = 1. \quad (2)$$

The g factor is a field breaking the $SO(5)$ symmetry into the $U(1)$ and $SO(3)$ subgroups, and is proportional to the doping rate in a loose sense [5].

The following notes on the above hamiltonian seem appropriate at this stage. First, the above hamiltonian can be considered as the Ginzburg-Landau description of the $SO(5)$ theory. Both of the AF and SC order parameters, \mathbf{s} and \mathbf{t} , are defined in a scale larger than the atomic one, but much smaller than the macroscopic one. In this sense they should be called as the local order parameters. The constraint (2) does not imply the existence of long-range order in the macroscopic scale. The long-range order parameter for the AF component is the staggered magnetization, and that for the SC component is the helicity modulus [16]. Second, although no quantum effect is included explicitly in hamiltonian (1), the competition between the two different long-range orders is taken into account sufficiently. Therefore, the profound, nontrivial thermodynamic properties of the $SO(5)$ theory can be captured. Third, thermal fluctuations in phase variables of SC order parameters, which are especially important for underdoped high- T_c cuprates [17], are taken into account by the first term in the above hamiltonian, and treated using the Monte Carlo technique. Furthermore, this hamiltonian is easily developed so as to incorporate an external magnetic field for the study of vortex states. Fourth, the superspin amplitude is fixed to unity in the above hamiltonian. The onset of superspin amplitude itself upon cooling can also be taken into account in the mean-field fashion, and is expected to correspond to the so-called pseudo-gap phenomenon [5]. Finally, only the simplest symmetry-breaking field g associated with the quadratic terms of order parameters is included in the hamiltonian. Other symmetry-breaking fields appear when high orders of the order parameters are considered [5,12]. Although an argument on magnitudes of these fields is

absent right now, it is reasonably expected that the most important features of the breaking of $SO(5)$ symmetry into the AF and SC subspaces are captured by the g field in (1).

A typical simulation process starts from a random configuration of superspins at a sufficiently high temperature. The system is then cooled gradually. The equilibrium state at a given temperature is generated using typically 50,000 MC sweeps of update from the state of a slightly higher temperature. In each sweep of update, candidate vectors are generated randomly on the five-dimensional unit sphere for superspins on all sites in the system, and are subject to the standard Metropolis algorithm to determine if they are accepted for the next configuration [18]. After this equilibration process, statistics on physical quantities is performed over 100,000 MC sweeps. Around transition temperatures, more than 10^6 MC sweeps are spent in order to make sure of sufficient equilibration and statistics. The system size for simulations in null external magnetic field is $L^3 = 40^3$, with periodic boundary conditions in all crystal directions. As the $SO(5)$ superspins are continuous in five dimensions, and the system is of three dimensions in crystal space, a thorough analysis of finite-size effects on simulation results, which is important for determining the relevant critical and bicritical exponents in high precisions, is extremely time consuming. Only for several chosen parameter sets, larger systems have been simulated in order to make sure that the main properties derived from the present simulations do not suffer from finite-size effects. Systematic errors (finite-size effects) are therefore not estimated for data presented in this paper. Statistical errors are comparable to sizes of marks in figures as far as not specified. The AF coupling in the ab plane $J_{ab}^{AF} \equiv J$ is taken as the energy unit, and temperature is measured by J/k_B throughout the present paper.

III. PHASE DIAGRAMS AND CORRELATION FUNCTIONS FOR $H = 0$

A. Isotropic system: $J_{ab}^{SC} = J_c^{SC} = J_c^{AF} = J_{ab}^{AF} \equiv J$

Figure 1 is the temperature vs. g -field phase diagram of the system with the same AF and SC coupling in all crystal directions. Both the N/AF and N/SC phase transitions are of second order, in the 3D Heisenberg and XY universality class, respectively. The two phase boundaries merge tangentially at the bicritical point $[g_b, T_b] = [0, 0.85J/k_B]$ [19]. For $g = g_b$ and $T > T_b$, the AF and SC correlation lengths for the two-point correlation functions are equal to each other, and isotropic in all crystal directions; the weights of AF and SC components are 3/5 and 2/5, proportional to the number of degrees of freedom. Away from the $SO(5)$ -symmetric line, positive (negative) g fields suppress AF (SC) correlations at all temperatures.

B. Anisotropic system: $J_{ab}^{SC} = 10J_c^{SC} = J_c^{AF} = J$

The temperature vs. g -field phase diagram of the system of couplings $J_{ab}^{SC} = J_c^{AF} = J$ and $J_c^{SC} = 0.1J$ is presented in Fig. 2. The bicritical point is at $[g_b, T_b] = [1.18J, 0.64J/k_B]$. The equal-weight partition of the superspin at $g = g_b$

observed in the isotropic system is broken. Nevertheless, as indicated in the inset of Fig. 2, in the ab plane the AF correlation length is equal to the SC correlation length when the g field is fixed at the bicritical value. This agreement is not trivial in contrast with the isotropic system. The SC correlation length in the c axis is much smaller than the other correlation lengths.

$$\text{C. Strongly anisotropic system: } 10J_{ab}^{SC} = 100J_c^{SC} = 100J_c^{AF} = J$$

In order to simulate real high- T_c cuprates, the AF exchange coupling should be taken much stronger than the effective SC coupling, and both AF and SC couplings are much weaker in the c axis. The temperature dependence of the AF staggered magnetization and the helicity modulus of the SC components [20] are shown in Fig. 3 for the system of couplings $J_{ab}^{SC} = 0.1J$ and $J_c^{SC} = J_c^{AF} = 0.01J$ at the symmetry breaking field $g = 1.96J$. Since the helicity modulus is proportional to the superfluid density [16], it is clear that the long-range SC order is established below the critical temperature $T_c \simeq 0.115J/k_B$. As shown in the same figure, the AF correlation length in the ab plane, ξ_{ab}^{AF} , increases at first as temperature is reduced, and then is suppressed as temperature approaches T_c . The maximal ξ_{ab}^{SC} is taken at the temperature $T_{sg} \simeq 0.15J/k_B$. The weight of AF components, $\langle s^2 \rangle$, decreases monotonically in the whole cooling process and shows a sharp decline among T_{sg} and T_c . Therefore, the enhancement of ξ_{ab}^{AF} above T_{sg} is clearly the result of reduction of thermal fluctuations; the suppression of ξ_{ab}^{AF} below T_{sg} is because of the loss of the AF order in its competition with the SC order. This peculiar behavior occurs because the AF coupling in the ab plane overwhelms over the SC one, while the SC groundstate is established by the large g field. Temperature dependence of the internal energy and the specific heat for this system are depicted in Fig. 4. No feature can be found around T_{sg} in these two thermodynamic quantities. Therefore, the only phase transition takes place at T_c , and T_{sg} corresponds merely to a crossover. The SC correlation length in the ab plane, ξ_{ab}^{SC} , diverges when temperature approaches T_c in Fig. 3, as usually in a thermodynamic second-order phase transition.

It is found experimentally that the spin-lattice relaxation rate assumes its maximum at a temperature well above the SC critical point [2]. The present simulation results indicate that this spin-gap phenomenon can be explained by the competition among the long-range SC and AF orders, and thermal fluctuations. Since the enhancement of AF correlations above the SC critical point is observed in the strongly anisotropic system of Fig. 3, but not in isotropic and slightly anisotropic systems of Figs. 1, and 2, it becomes clear that in order to observe the spin-gap behavior, the system should have SC couplings much weaker than AF ones, as in real high- T_c cuprates.

Figure 5 is the temperature vs. g -field phase diagram of the same couplings for Figs. 3 and 4. The bicritical point is at $[g_b, T_b] = [1.93J, 0.12J/k_B]$. The latent heat associated with the first-order transition between the AF and SC phases is approximately $Q \simeq 0.05J$, and decreases to zero as the bicritical point is approached. The spin-gap like phenomenon is observed in the region $g_b < g < 2.2J$. For $g > 2.2J$, AF correlations are suppressed by SC components at all temperatures. The experimental fact that spin-gap behaviors are observed only in the underdoped region of high- T_c cuprates may be explained by the present simulation result. The ratio between the spin-gap temperature and

the SC critical point is $T_{sg}/T_c \simeq 1.6$ at $g = 2J$, which counts well the experimental observation [2].

In Fig. 5, the spin-gap temperature T_{sg} decreases as the bicritical point is approached. This might seem curious at a first glance, since it is clear from hamiltonian (1) that the larger the g field the smaller the AF components. Shown in Figs. 6 (A) and (B) are the temperature dependence of the AF correlation length and the staggered susceptibility at several g fields. Although both of them are monotonically suppressed by increasing g field when temperature is fixed, the temperature where they take maxima, T_{sg} , increases with the g field, as clearly seen in Figs. 6. It is noted that the spin-gap temperature increases with decreasing doping rate in experiments. The present theory therefore conflicts with experimental observations in this aspect.

The SC correlations are suppressed in the normal state above the AF phase boundary in the present system. In this sense, there is no counterpart of the spin-gap temperature above Néel points. However, it is interesting to observe in Fig. 7 that for the g field in a certain region below the bicritical value, the SC weight, $\langle t^2 \rangle$, takes maximum at a temperature above the corresponding Néel point. The temperature associated with the maximal SC weight, denoted by T_p in Fig. 5, may be identified with the pairing temperature [5]. There is no feature in the internal energy and the specific heat around this crossover temperature.

IV. PHASE DIAGRAM AND VORTEX STATES FOR $H > H_{C1}$

A. Model hamiltonian and phase diagram

An external magnetic field penetrates into a type-II superconductor via thin flux lines associated with flux quanta for H larger than the lower critical field H_{c1} . SC is broken along the flux lines. High- T_c superconductors are extremely type-II with very large Ginzburg-Landau numbers $\kappa \sim 100$. Research of the vortex states in high- T_c SC has been growing into a vivid field of condensed matter physics and statistics. The most important feature of the vortex states is that the Abrikosov FLL melts into FL liquid via a first-order phase transition [21,22,20].

In the scheme of the $SO(5)$ theory, the free energy of a vortex state can be reduced by rotating the superspins from the SC subspace into the AF subspace at the flux-line cores [5]. The possibility of AF cores of flux lines in the $SO(5)$ theory was first addressed by Arovas *et al.* [8]. Recently, Alama *et al.* discussed the κ dependence of the core state [15]. In these studies, the Abrikosov mean-field theory was developed so as to incorporate the AF components. However, the Abrikosov mean-field theory for the vortex states is not appropriate for the high- T_c SC since it only takes into account the amplitude of SC order parameter, and cannot treat thermal fluctuations in the phase variables, which are essentially important for determining the phase diagram of the vortex states in high- T_c SC [20].

The hamiltonian for the $SO(5)$ theory in the presence of an external magnetic field may be given as following [13]:

$$\mathcal{H} = - \sum_{\langle i,j \rangle} J_{ij}^{SC} |\mathbf{t}_i| |\mathbf{t}_j| \cos(\varphi_i - \varphi_j - A_{ij}) + \sum_{\langle i,j \rangle} J_{ij}^{AF} \mathbf{s}_i \cdot \mathbf{s}_j - \sum_i \mathbf{H} \cdot \mathbf{s}_i + g \sum_i \mathbf{s}_i^2, \quad A_{ij} = \frac{2\pi}{\phi_0} \int_i^j \mathbf{A} \cdot d\mathbf{r}, \quad (3)$$

where $|\mathbf{t}|$ and φ are the amplitude and phase of the SC order parameter. The same constraint (2) is applied. Fluctuations of the magnetic induction are neglected. This approximation is justified when the separation between

vortices is larger than the SC correlation length and much smaller than the penetration depth in the ab plane, a condition satisfied in large portion of $H - T$ phase diagrams of high- T_c superconductors. The Josephson coupling should also be dominant over the electromagnetic coupling. The first term in the above hamiltonian, known as the fully frustrated 3D XY model, has been used successfully for explaining many important thermodynamic properties of the vortex states in high- T_c SC [20,23].

In order to simplify the situation, the case of an external magnetic field parallel to the c axis is addressed in the present paper [23]. The vector potential is given by $\mathbf{A} = (-yB/2, xB/2, 0)$ with $B = f\phi_0/l_{ab}^2$. Here, ϕ_0 is the flux quantum, l_{ab} the unit length in the ab plane, and f the average number of flux in each square unit cell in the ab plane. The data shown in the following are for $f = 1/25$, corresponding to the inter-vortex distance of $d_v = \sqrt{2/\sqrt{3}}l_{ab}/\sqrt{f} \simeq 5.37l_{ab}$ in the triangular FLL. The system size is chosen as $L_a \times L_b \times L_c = 50 \times 50 \times 40$ with periodic boundary conditions in all crystal directions [20]. Although the relation between the magnetic induction B and the Zeeman field H is not clear, the value of the Zeeman field is not much relevant to the following discussions, and thus is fixed to $H = 0.1J$. In the present approach, vortices are defined by topological singularities in the configuration of phase variables of SC order parameters: $\sum_{\text{cell}}(\varphi_i - \varphi_j - A_{ij}) = (n - f)2\pi$, where n is the vorticity.

The temperature vs. g -field phase diagram of the system with couplings $J_{ab}^{SC} = J_c^{AF} = J$ and $J_c^{SC} = 0.1J$ is depicted in Fig. 8. There are three ordered phases, namely the AF phase, AF and FLL coexistence phase, and FLL phase. The onset of long-range SC order is a first-order phase transition, same as those in systems of no AF components [20]: At the melting temperature T_m the FL liquid is frozen into the triangular FLL; the helicity modulus along the c axis jumps sharply from zero to a finite value; there is a δ -function peak in the specific heat, associated with a small latent heat. The onset of the long-range AF order is always a second-order phase transition [24].

From the comparison between the two phase diagrams in Figs. 2 and 8 of same couplings, it is clear that suppression of the transition temperature of the long-range SC order by the external magnetic field is much more significant than that of the long-range AF order. This difference is understood easily considering the structures of these two long-range orders: For the long-range AF order, the magnetic spins are aligned antiferromagnetically, almost within the ab plane. This configuration reduces the influence of the magnetic field on the onset of long-range AF order. On the other hand, the external magnetic field induces flux lines in the SC state, and produces strong fluctuations in phase variables of SC order parameters. The long-range SC order is established only when the flux lines are frozen into FLL. The above difference in the magnetic-field responses results also in the expansion of the AF phase into the SC territory, as can be seen in Figs. 2 and 8.

In the region $1.0J \leq g \leq 1.32J$, the long-range AF and SC orders coexist at low temperatures. The temperature dependence of the helicity modulus along the c axis, the staggered magnetization, and the specific heat are shown in Fig. 9 for $g = 1.1J$. The N/AF transition at T_N is a thermodynamic second-order phase transition, above the first-order onset of the long-range SC order at T_m . Although suppressed by the SC order in certain degree, the staggered magnetization survives to groundstate.

The AF phase boundary drops sharply from $[g, T] = [1.32J, 0.59J/k_B]$ in Fig. 8. The phase transition at this

almost vertical part of AF phase boundary is investigated by tuning the g field at a fixed temperature, in addition to the cooling process mentioned in Sec. II. The turning point on the N/AF phase boundary in Fig. 8 and the tricritical point in Ref. [13] are at the same temperature.

B. AF vortex cores

The vortex cores in the SC phase of the $SO(5)$ theory are different from those without AF competition studied up to date. The structure factors $S(\mathbf{q}_{ab}, z=0)$ for vortices, s^2 , s_{ab} , and s_c for $g = 1.5J$ in the FLL phase are displayed in Figs. 10. The Bragg peaks in the structure factor Fig. 10(A) for the vortex correlations are from the triangular FLL. One also finds Bragg peaks in structure factor Fig. 10(B) for the AF amplitudes at the same wave numbers of Fig. 10(A). This coincidence indicates clearly that cores of flux lines are of larger AF weights than elsewhere. The g -field dependence of the Bragg-spot height for AF weights in the FLL phase, such as those in Fig. 10(B), is investigated when temperature is fixed. As shown in Fig. 11 for $T = 0.3J/k_B$, $S(\mathbf{q}_{ab} = \mathbf{q}_{max}, z=0)$ decays with increasing g field in a power law $S \simeq p/g^q$ with $p = 0.8 \pm 0.05$ and $q = 3 \pm 0.1$. The haloes at the wave numbers $Q = (\pm\pi, \pm\pi)$ in the structure factors for s_{ab} and s_c in Figs. 10(C) and (D) correspond to short-range AF fluctuations. The weak spot at $Q = (0, 0)$ in Fig. 10(D) is from the small ferromagnetic component s_c induced by the external magnetic field.

The structure factors $S(\mathbf{q}_{ab}, z=0)$ in the AF and FLL coexistence phase for vortices, s^2 , s_{ab} , and s_c are displayed in Figs. 12. From the structure factors Figs. 12(A) and (B) for vortices and AF amplitudes, it is clear that AF components are enhanced in cores of flux lines, as in the FLL phase. In structure factors Figs. 12(C) and (D) for s_{ab} and s_c , there are strong Bragg peaks at $Q = (\pm\pi, \pm\pi)$ associated with the long-range AF order. Satellite spots are observed around the main Bragg peaks in Figs. 12(C) and (D). These satellite spots are easily identified with those in Figs. 12(A) and (B). Therefore, in the AF and FLL coexistence phase, the phase of the long-range AF order is preserved in cores of flux lines.

V. SUMMARY

Thermodynamic properties of the $SO(5)$ theory are investigated using Monte Carlo simulations on a model hamiltonian which counts thermal fluctuations both in the rotations of superspins between the SC and AF subspaces, and in the phase variables of the SC order parameters. The latter factor is essentially important for explaining thermodynamic phase transitions associated with the onset of long-range SC order in high- T_c cuprates in null and finite external magnetic fields. Therefore, the present approach is superior to Abrikosov-type mean-field treatments of the $SO(5)$ theory, in which thermal fluctuations in the phases of SC order parameters are neglected.

For null external magnetic field, there is a bicritical point in the temperature vs. g -field phase diagram, at which the second-order N/AF and N/SC phase boundaries merge tangentially into the first-order AF/SC phase boundary. Hysteresis phenomenon is observed at the first-order AF/SC phase transition, which may suggest a phase-separation

region in the phase diagram.

In systems with much stronger AF couplings than SC ones while the SC groundstate is achieved by g fields larger than the bicritical value, AF correlations are enhanced at a crossover temperature above the SC critical point. The origin of this enhancement in AF correlations is clarified to be the competition among the long-range AF and SC orders and thermal fluctuations. When the g field becomes too large, this crossover fades away since AF correlations are suppressed at all temperatures by the large SC component. These results are consistent with the spin-gap phenomenon observed experimentally in the following aspects: First, real cuprates are very anisotropic in the AF and SC couplings $J^{AF} \sim 0.1$ eV and $J^{SC} \sim 0.01$ eV; Second, the spin-gap phenomenon has been observed experimentally only in the underdoped region. In contrast with experimental observations, however, the spin-gap temperature decreases as the bicritical point is approached from the SC side. Near the bicritical point, there is a crossover temperature above the Néel temperature where the weight of SC components takes maximum.

The $SO(5)$ theory in an external magnetic field is also investigated. The long-range SC order is established through a first-order freezing transition from the FL liquid into the FLL, while the onset of the long-range AF order is associated with a second-order phase transition. These two phase boundaries cross each other, and thus produce a region in the phase diagram where the two long-range orders coexist. In the FLL phase, only short-range AF fluctuations are enhanced at cores of flux lines. 1D long-range AF order along the flux line cannot be realized because of strong thermal fluctuations. In the coexistence phase, superlattice spots surrounding the strong AF Bragg peaks at $Q = (\pm\pi, \pm\pi)$ are observed in the simulated structure factor, and are identified with the modulation by the triangular flux-line lattice of SC. This simulation result can be checked by the neutron scattering technique.

Acknowledgements

The author would like to thank S.-C. Zhang, T. Koyama, and Y. K. Bang for stimulating conversations on the $SO(5)$ theory. M. Tachiki is very grateful for drawing author's attention to vortex states in high- T_c superconductivity and continuous encouragement. He appreciates S. Miyashita, N. Akaiwa, M. Itakura, and Y. Nonomura for helpful discussions on technical points of MC simulation. The present simulations are performed on the Numerical Materials Simulator (SX-4) of National Research Institute for Metals (NRIM), Japan.

-
- [1] J. G. Bednorz and K. A. Müller, Z. Phys. B **64**, 189 (1986).
 - [2] H. Yasuoka, Y. Imai and T. Shimizu, *Springer Series in Solid State Science 89, Strong Correlation and Superconductivity*, ed. H. Fukuyama, S. Maekawa and A. P. Malozemoff (Springer-Verlag, New York, 1989) 254.
 - [3] P. W. Anderson, Science **235**, 1196 (1987); *The theory of superconductivity in the high- T_c cuprates*, (Princeton Univ. Press, New Jersey, 1997).
 - [4] F. C. Zhang and T. M. Rice, Phys. Rev. B **37**, 3759 (1988).
 - [5] S.-C. Zhang, Science **275**, 1089 (1997).
 - [6] E. Demler and S.-C. Zhang, Phys. Rev. Lett. **75**, 4126 (1995).
 - [7] S. Meixner, W. Hanke, E. Demler, and S.-C. Zhang, Phys. Rev. Lett. **79**, 4902 (1997).
 - [8] D. P. Arovas, A. J. Berlinsky, C. Kallin, and S.-C. Zhang, Phys. Rev. Lett. **79**, 2871 (1997).
 - [9] T. Koyama, J. Phys. Soc. Jpn. **66**, 4051 (1997); *Adv. in Superconductivity X*, edited by K. Osamura and I. Hirabayashi, (Springer-Verlag, Tokyo, 1998), 257.
 - [10] S. Rabello, H. Kohno, E. Demler, and S.-C. Zhang, Phys. Rev. Lett. **80**, 3586 (1998).
 - [11] C. L. Henley, Phys. Rev. Lett. **80**, 3590 (1998).
 - [12] R. Eder, W. Hanke, and S.-C. Zhang, Phys. Rev. B **57**, 13781 (1998).
 - [13] X. Hu, T. Koyama, and M. Tachiki, Phys. Rev. Lett. **82**, 2568(1999).
 - [14] S. Murakami, N. Nagaosa, and M. Sigrist, Phys. Rev. Lett. **82**, 2939 (1999).
 - [15] S. Alama, A. J. Berlinsky, L. Bronsard, and T. Giorgi, cond-mat/9812283.
 - [16] M. E. Fisher, M. N. Barber, and D. Jasnow, Phys. Rev. A **8**, 1111 (1973).
 - [17] V. J. Emery and S. A. Kivelson, Nature (London) **374**, 434 (1995).
 - [18] In Ref. [13], candidates of superspins are generated with the same SC and AF weight, 1/2, in average. When a superspin is generated randomly in a five-dimensional unit sphere as in the present paper, the SC and AF weight should be 2/5 and 3/5, respectively. In this sense, there was a bias field favoring the SC order in the system in Ref. [13]. The temperature vs. g -field phase diagrams should be compared with each other by shifting the g axis with a certain amount.
 - [19] M. E. Fisher and D. R. Nelson, Phys. Rev. Lett. **32**, 1350 (1974); D. R. Nelson, J. M. Kosterlitz, and M. E. Fisher, Phys. Rev. Lett. **33**, 813 (1974).

- [20] X. Hu, S. Miyashita, and M. Tachiki, Phys. Rev. Lett. **79**, 3498 (1997); Phys. Rev. B **58**, 3438 (1998); references therein.
- [21] G. Blatter *et al*, Rev. Mod. Phys. **66** , 1125 (1994).
- [22] G. W. Crabtree and D. R. Nelson, Physics Today **45**, 39 (1997).
- [23] X. Hu and M. Tachiki, Phys. Rev. Lett. **80**, 4044 (1998).
- [24] This observation is different from that reported in Ref. [13], where there is a tricritical point on the N/AF phase boundary at $[g_t, T_t] = [0.40J, 0.59J/k_B]$; there is a region at $g > g_t$ where the N/AF phase transition is of first order. This discrepancy comes from the different ways of generation of superspins [18].

Figure Captions

Fig. 1: Temperature vs. g -field phase diagram of the system with isotropic AF and SC couplings. The bicritical point is at $[g_b, T_b] = [0, 0.85J/k_B]$.

Fig. 2: Temperature vs. g -field phase diagram of the system with the couplings $J_{ab}^{SC} = J_c^{AF} = J$, and $J_c^{SC} = 0.1J$. The bicritical point is at $[g_b, T_b] = [1.18J, 0.64J/k_B]$. Inset: temperature dependence of the AF and SC correlation lengths in the ab plane at $g = g_b$.

Fig. 3: Temperature dependence of the AF and SC order parameters, correlation lengths, and the weight of AF components at $g = 1.96J$ in the system with couplings $J_{ab}^{SC} = 0.1J$ and $J_c^{SC} = J_c^{AF} = 0.01J$. Here, T_c is the SC transition point, and T_{sg} is the spin-gap temperature.

Fig. 4: Temperature dependence of the internal energy and the specific heat per site for the same system in Fig. 3.

Fig. 5: Temperature vs. g -field phase diagram for the same couplings in Fig. 3. The bicritical point is at $[g_b, T_b] = [1.93J, 0.12J/k_B]$. The spin-gap temperature T_{sg} and pairing temperature T_p fade away around $g = 2.2J$ and $g = 1.5J$ respectively.

Fig. 6: Temperature dependence of the AF correlation length in the ab plane (A) and the staggered susceptibility (B) at several typical g fields. Maxima are assumed at the spin-gap temperatures T_{sg} for $g > g_b = 1.93J$.

Fig. 7: Temperature dependence of the SC weight at a series of g fields. Maxima are assumed at the pairing temperatures T_p for $1.5J < g < g_b$.

Fig. 8: Temperature vs. g -field phase diagram of the system with the couplings $J_{ab}^{SC} = J_c^{AF} = J$ and $J_c^{SC} = 0.1J$. The flux density is given by $f = 1/25$, and the Zeeman field is $H = 0.1J$.

Fig. 9: Temperature dependence of the helicity modulus along the c axis, the staggered magnetization, and the specific heat per site in the system of the same couplings of Fig. 8 at $g = 1.1J$.

Fig. 10: Structure factors $S(\mathbf{q}_{ab}, z = 0)$ for vortices (A), s^2 (B), s_{ab} (C), and s_c (D) in the FLL phase in Fig. 8.

Fig. 11: g -field dependence of the Bragg-spot height for the AF weights at $T = 0.3J/k_B$.

Fig. 12: Structure factors $S(\mathbf{q}_{ab}, z = 0)$ for vortices (A), s^2 (B), s_{ab} (C), and s_c (D) in the AF and FLL coexistence phase in Fig. 8.

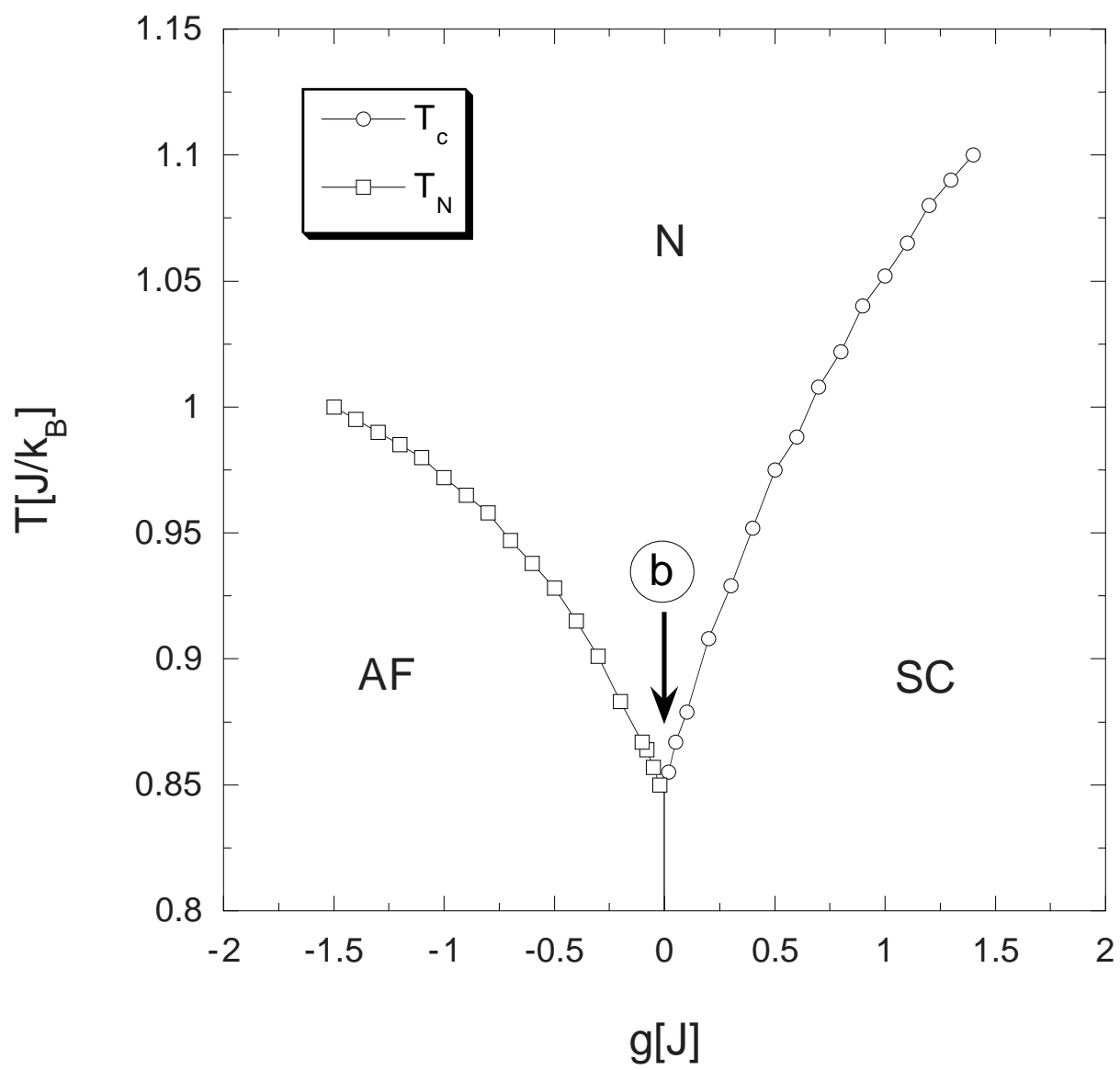
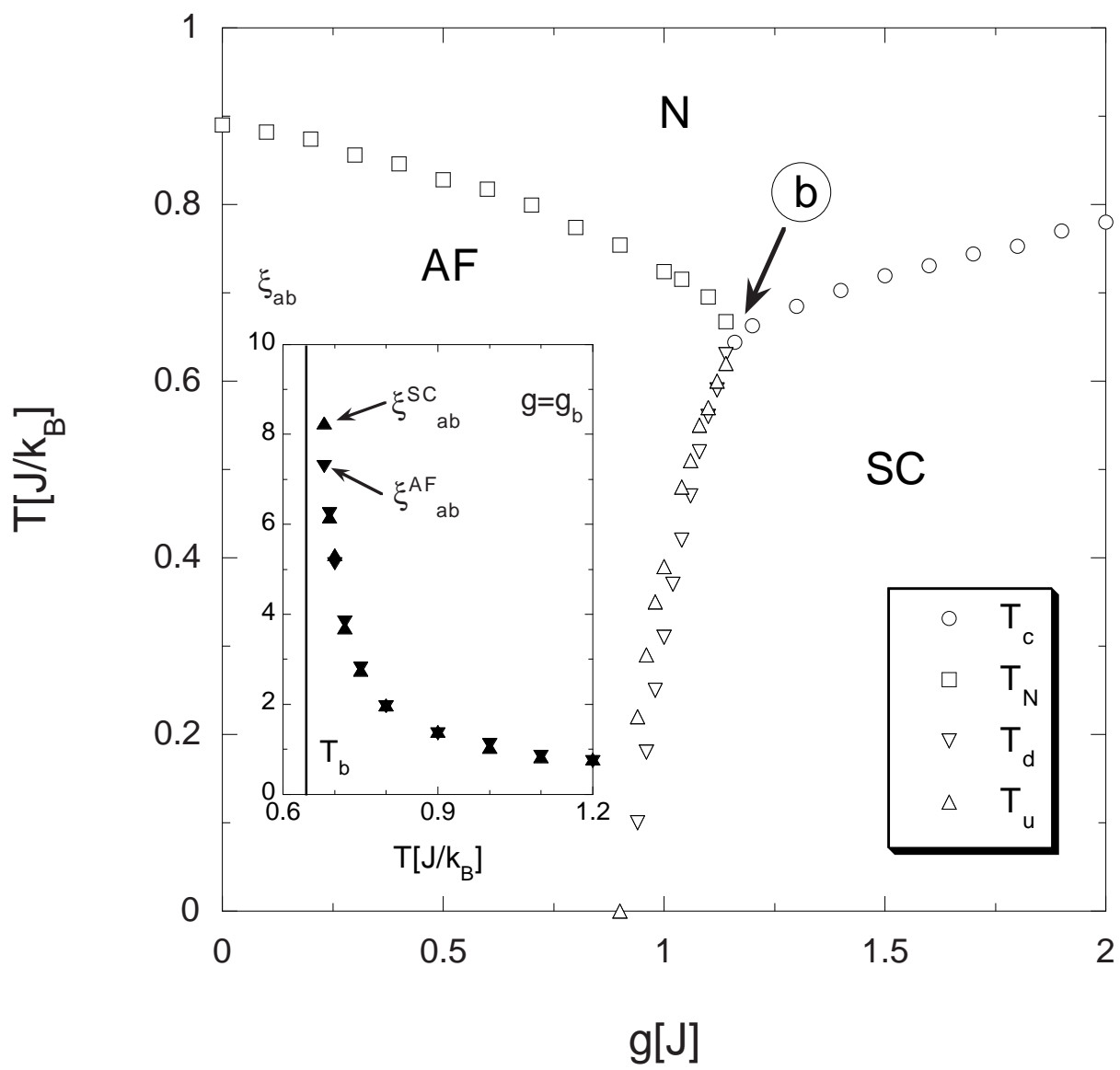


Fig.1 by Xiao HU



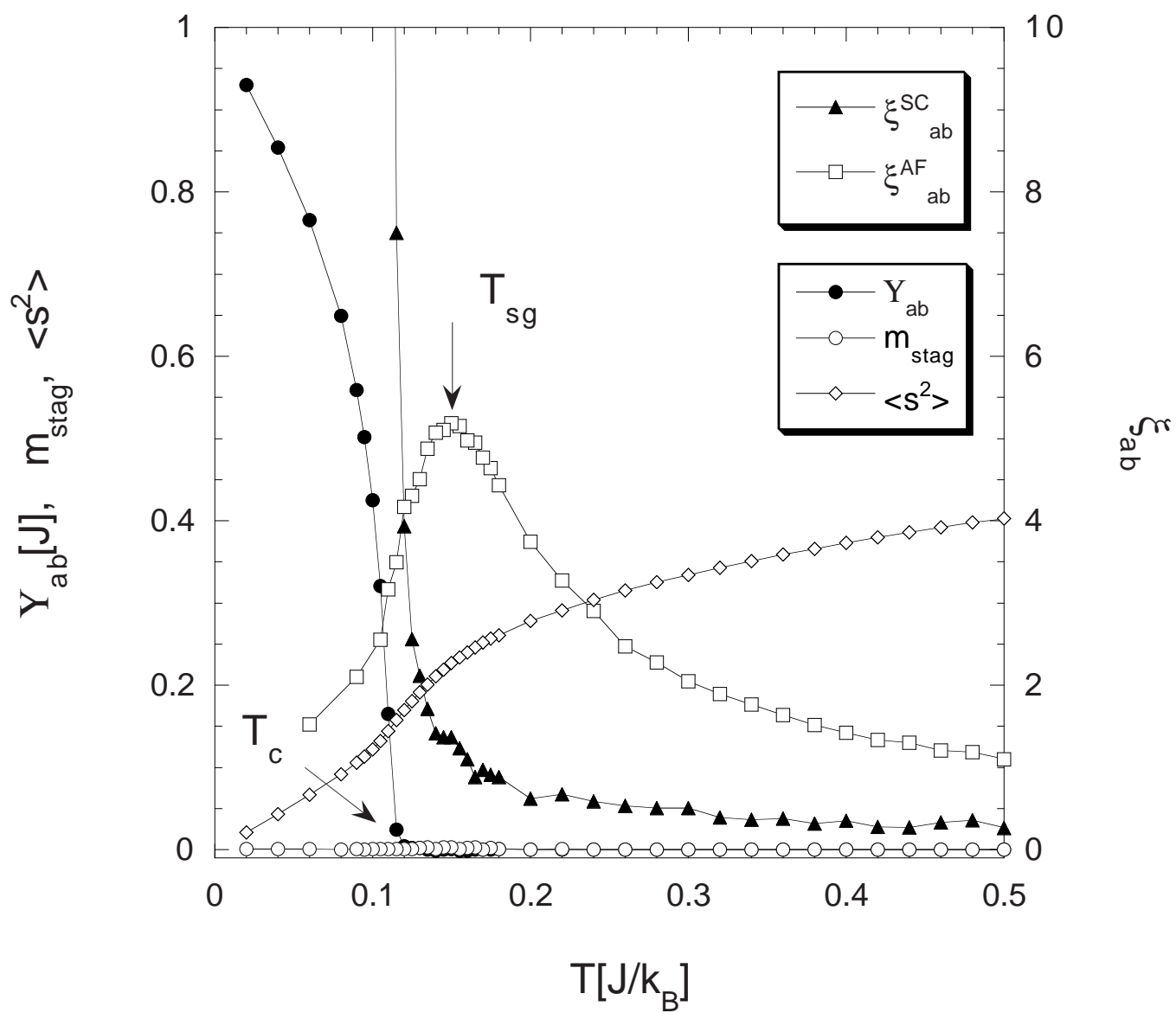


Fig.3 by Xiao HU

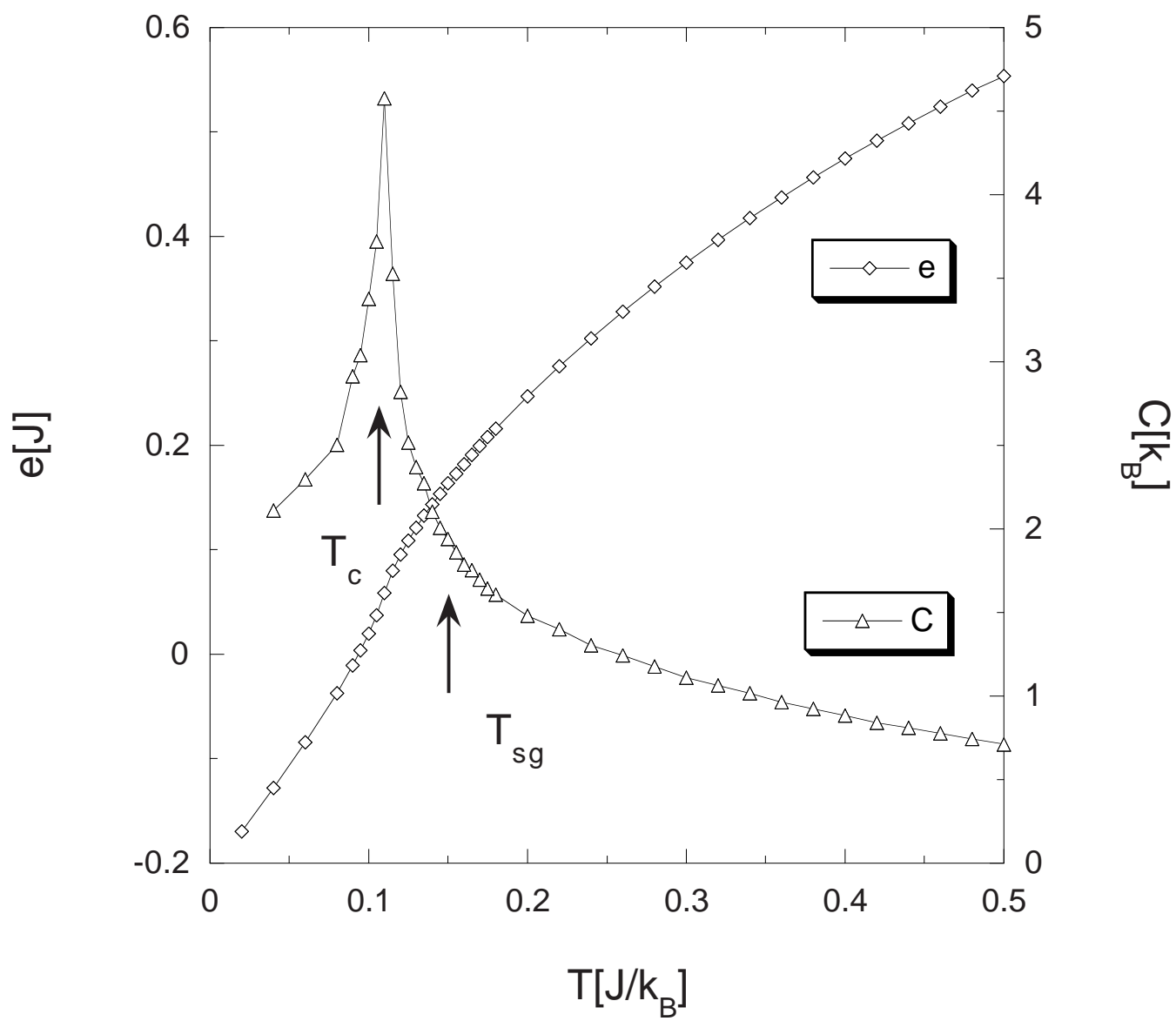


Fig.4 by Xiao HU

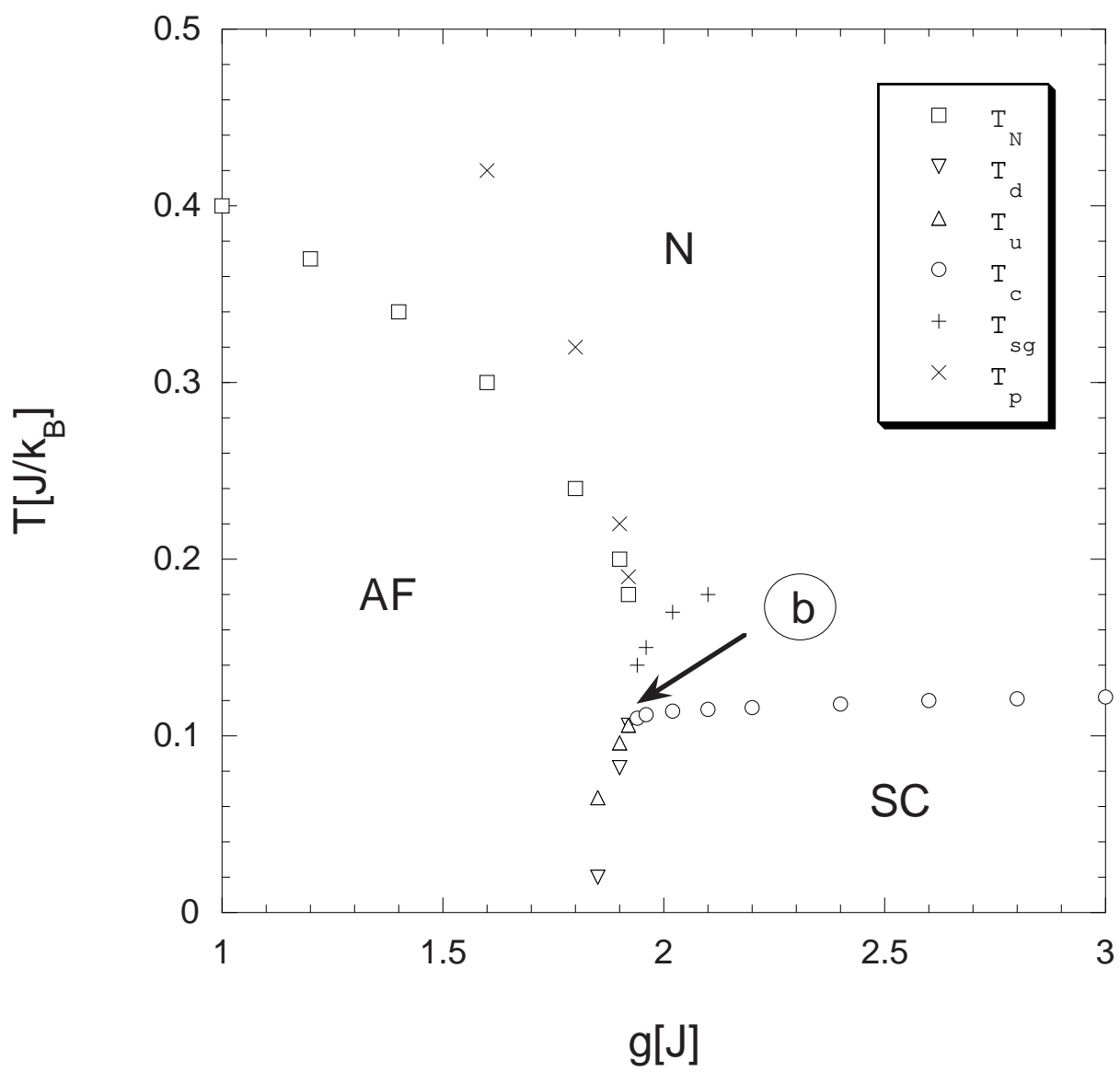


Fig.5 by Xiao HU

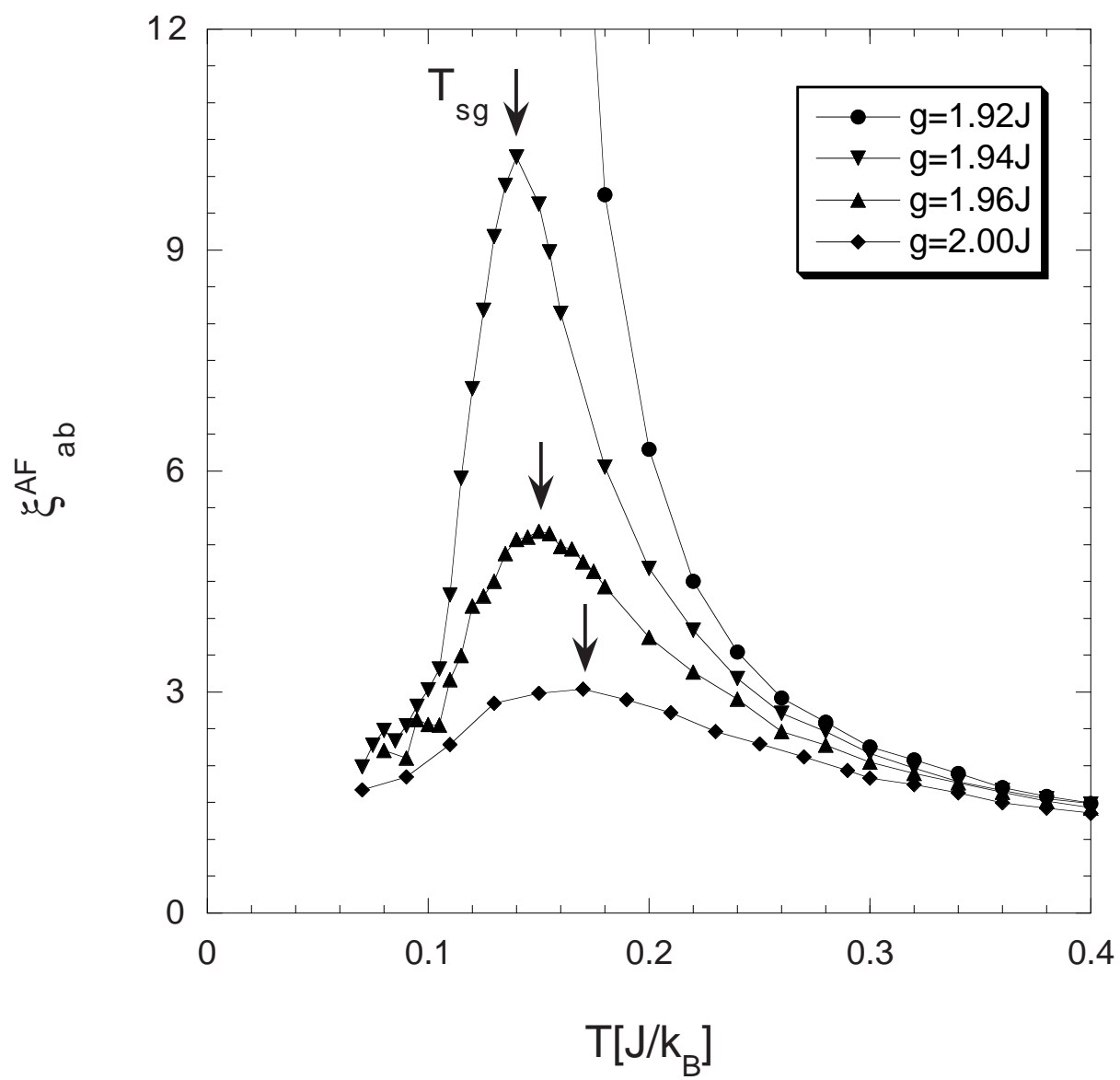


Fig.6(A) by Xiao HU

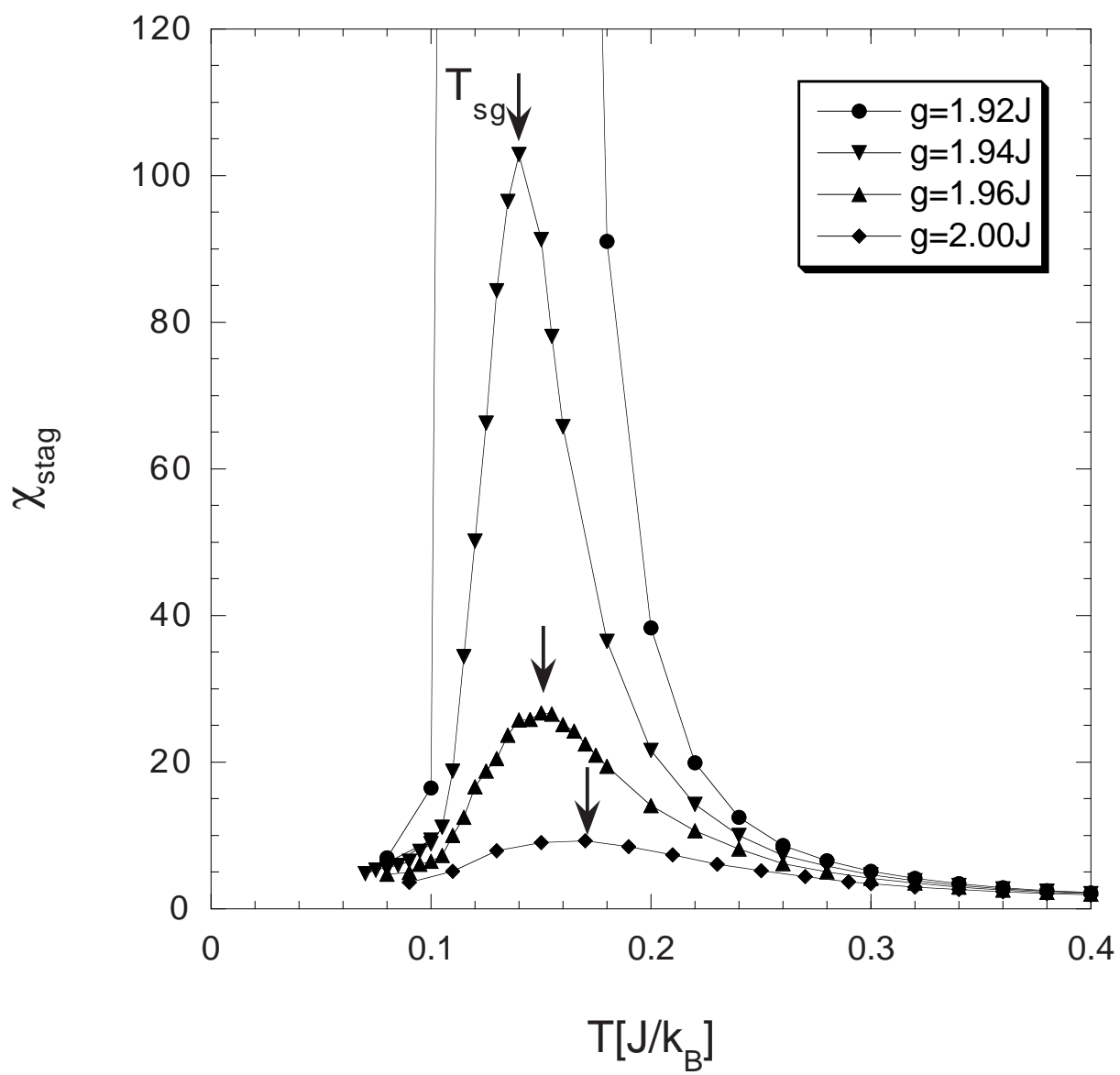


Fig.6(B) by Xiao HU

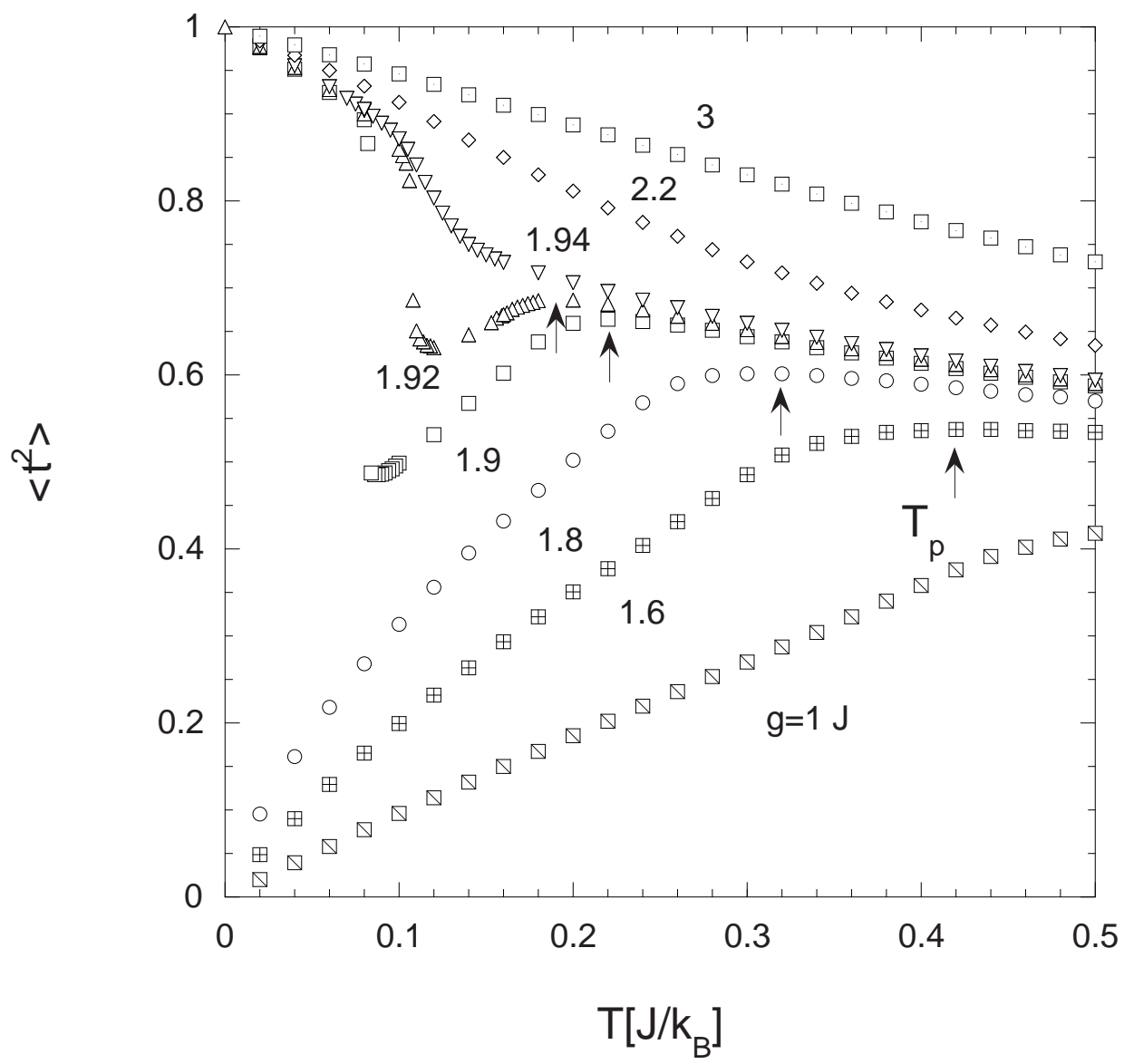


Fig.7 by Xiao HU

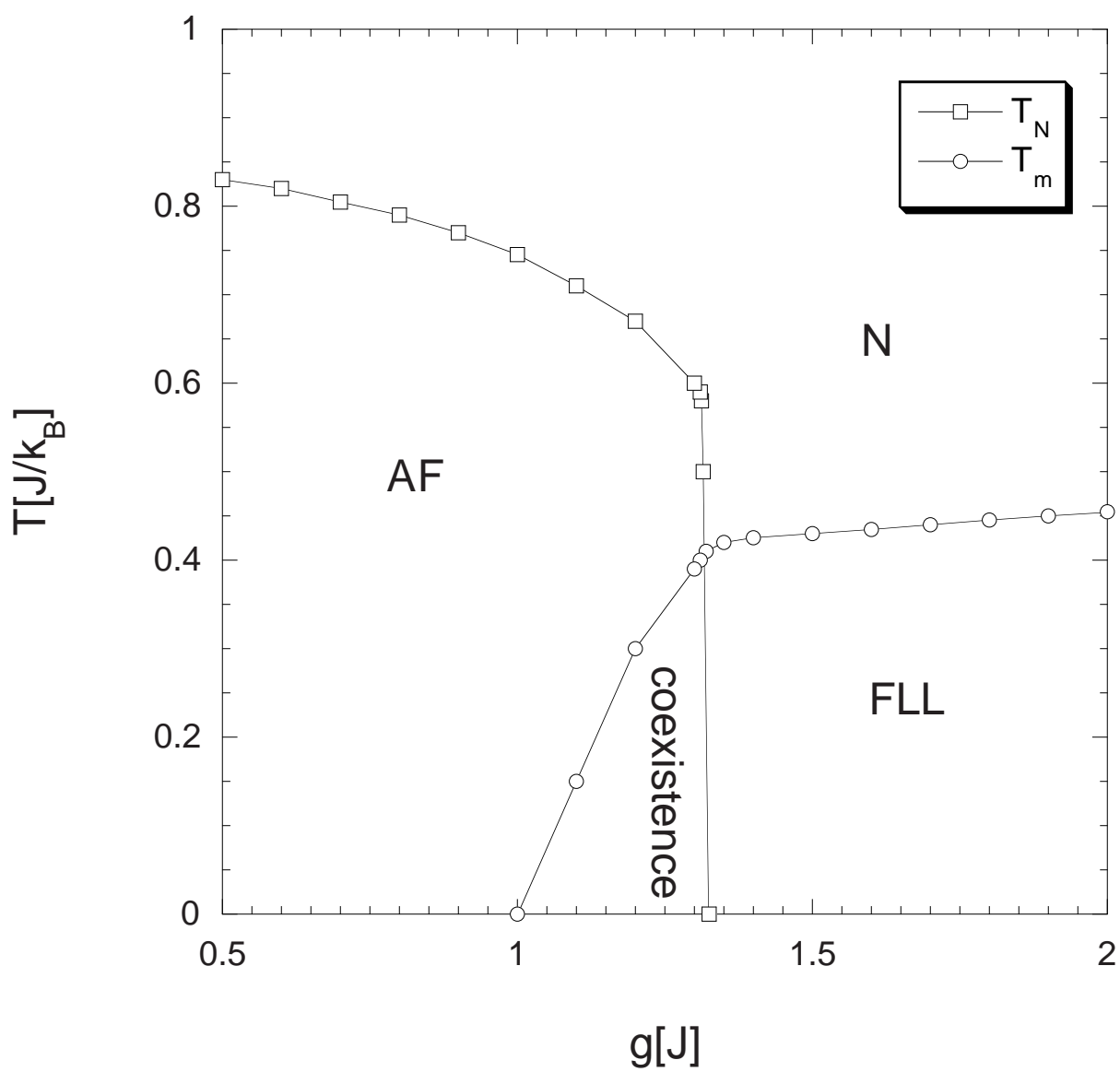


Fig.8 by Xiao HU

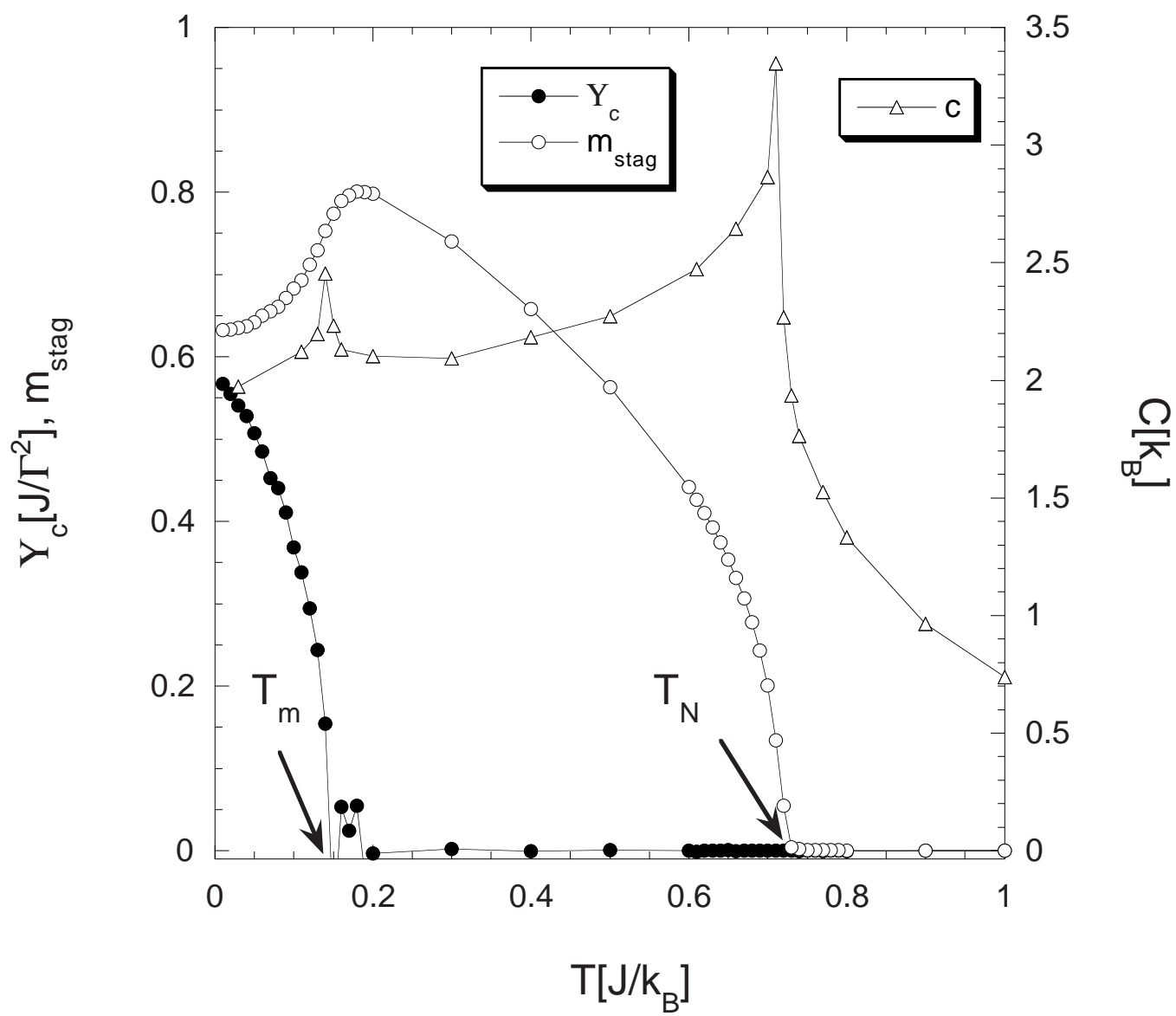
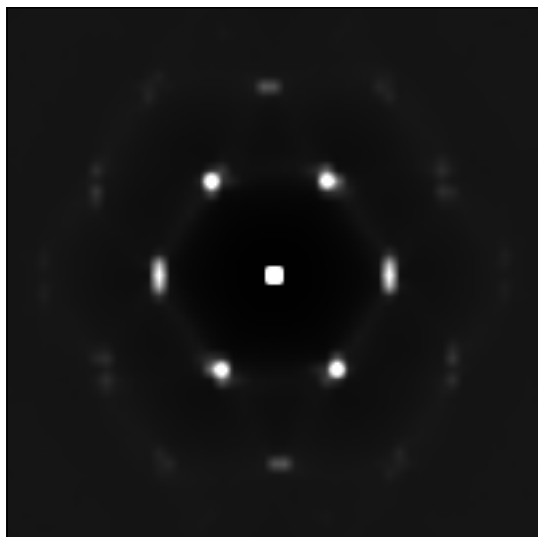
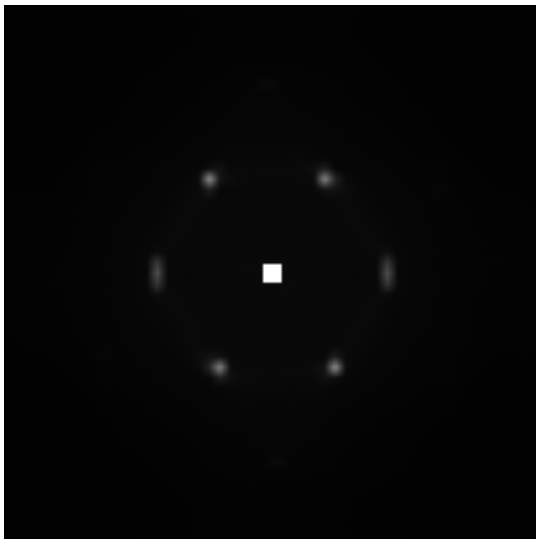
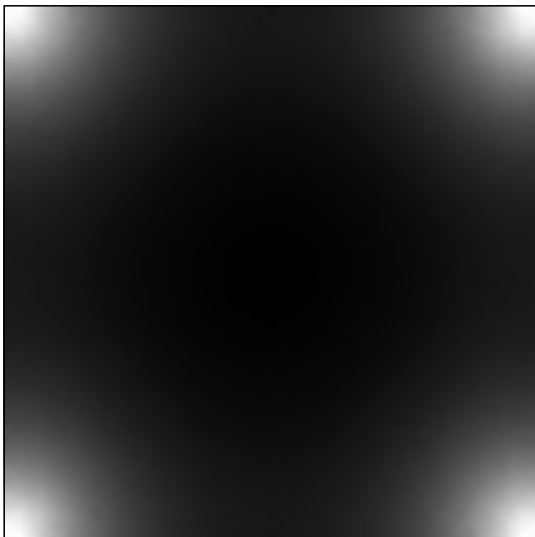
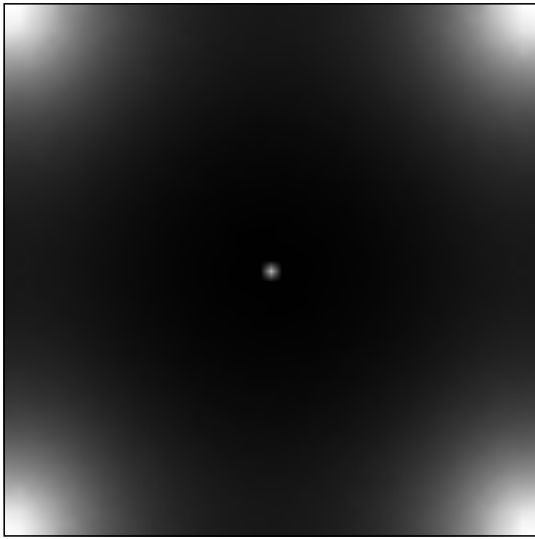


Fig.9 by Xiao HU









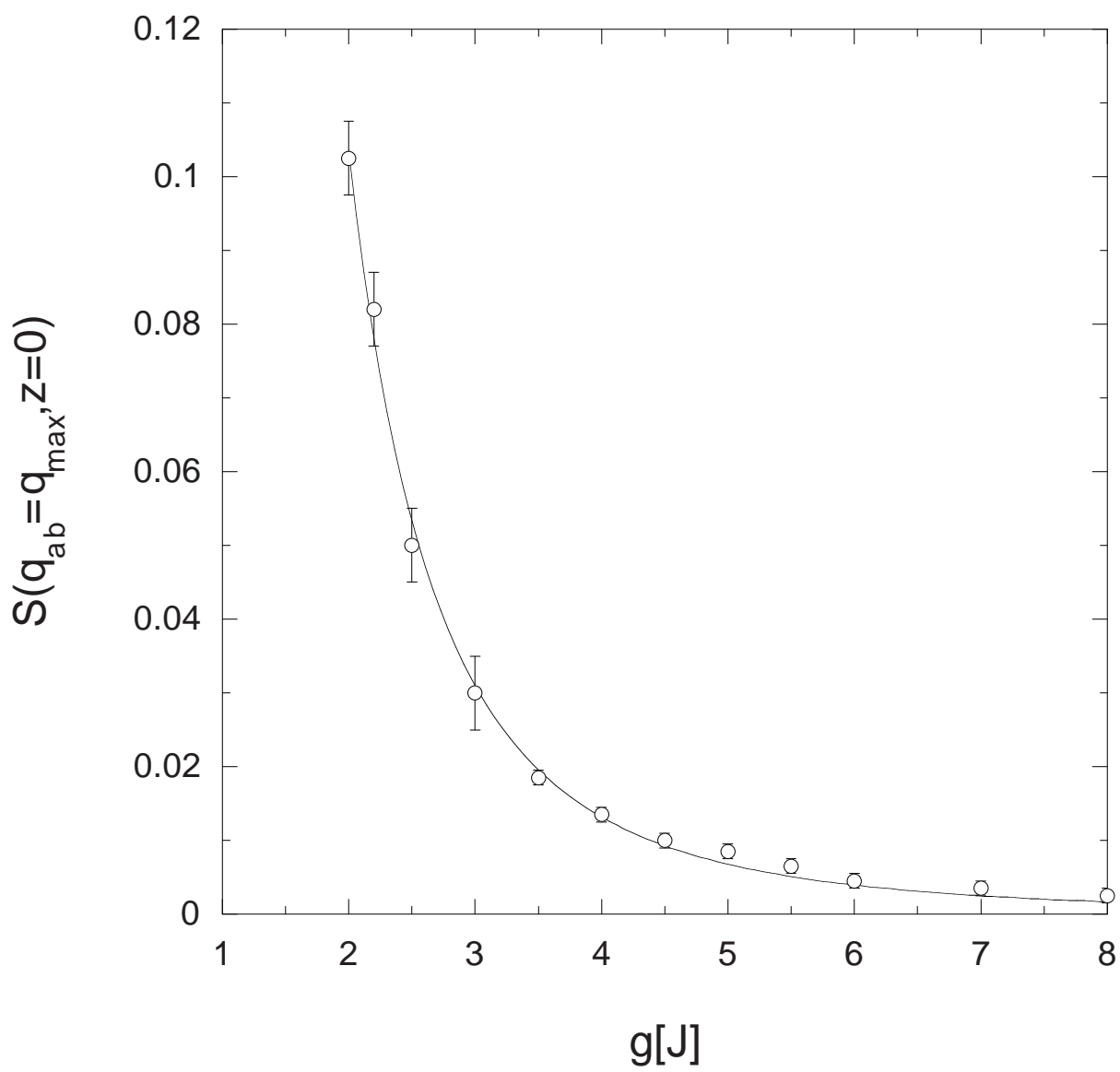


Fig.11 by Xiao HU

